11-15-1996

Structure of the GDP-Pi complex of Gly203→Ala G(iα1): a mimic of the ternary product complex of Galpha-catalyzed GTP hydrolysis

Albert M. Berghuis
University of Texas at Dallas

Ethan Lee
University of Texas Southwestern Medical Center

André S. Raw
University of Texas Southwestern Medical Center

Alfred G. Gilman
University of Texas Southwestern Medical Center

Stephen R. Sprang
University of Montana, stephen.sprang@umontana.edu

Structure of the GDP–Pi complex of Gly203→Ala $G_{i\alpha1}$: a mimic of the ternary product complex of Gα-catalyzed GTP hydrolysis

Albert M Berghuis[1†], Ethan Lee[2], André S Raw[2], Alfred G Gilman[2] and Stephen R Sprang[1,3*]

Background: G proteins play a vital role in transmembrane signalling events. In their inactive form G proteins exist as heterotrimers consisting of an α subunit, complexed with GDP and a dimer of βγ subunits. Upon stimulation by receptors, G protein α subunits exchange GDP for GTP and dissociate from βγ. Thus activated, α subunits stimulate or inhibit downstream effectors. The duration of the activated state corresponds to the single turnover rate of GTP hydrolysis, which is typically in the range of seconds. In $G_{i\alpha1}$, the Gly203→Ala mutation reduces the affinity of the substrate for Mg^{2+}, inhibits a key conformational step that occurs upon GTP binding and consequently inhibits the release of βγ subunits from the GTP complex. The structure of the Gly203→Ala mutant of $G_{i\alpha1}$ ($G203AG_{i\alpha1}$) bound to the slowly hydrolyzing analog of GTP (GTPγS) has been determined in order to elucidate the structural changes that take place during hydrolysis.

Results: We have determined the three dimensional structure of a Gly203→Ala mutant of $G_{i\alpha1}$ at 2.6 Å resolution. Although crystals were grown in the presence of GTPγS and Mg^{2+}, the catalytic site contains a molecule of GDP and a phosphate ion, but no Mg^{2+}. The phosphate ion is bound to a site near that occupied by the γ-phosphate of GTPγS in the activated wild-type α subunit. A region of the protein, termed the Switch II helix, twists and bends to adopt a conformation that is radically different from that observed in other $G_{i\alpha1}$ subunit complexes.

Conclusions: Under the conditions of crystallization, the Gly203→Ala mutation appears to stabilize a conformation that may be similar, although perhaps not identical, to the transient ternary product complex of $G_{i\alpha1}$-catalyzed GTP hydrolysis. The rearrangement of the Switch II helix avoids a potential steric conflict caused by the mutation. However, it appears that dissociation of the γ-phosphate from the pentacoordinate intermediate also requires a conformational change in Switch II. Thus, a conformational rearrangement of the Switch II helix may be required in Gα-catalyzed GTP hydrolysis.

Addresses: [1]Howard Hughes Medical Institute, The University of Texas Southwestern Medical Center, 5323 Harry Hines Blvd., Dallas, TX 75235-9050, USA, [2]Department of Pharmacology The University of Texas Southwestern Medical Center, 5323 Harry Hines Blvd., Dallas, TX 75235-9050, USA and [3]Department of Biochemistry, The University of Texas Southwestern Medical Center, 5323 Harry Hines Blvd., Dallas, TX 75235-9050 USA.

[†]Present address: Department of Biochemistry, McMaster University, 1200 Main Street West, Hamilton, Ontario L8N 3Z5, Canada.

*Corresponding author.
E-mail: sprang@howie.swmed.edu

Key words: enzyme mechanism, G proteins, protein tertiary structure

Received: 29 July 1996
Revisions requested: 27 August 1996
Revisions received: 11 September 1996
Accepted: 11 September 1996

Structure 15 November 1996, 4:1277–1290

 ISSN 0969-2126

Introduction

G protein mediated transmembrane signaling has been well characterized from a biochemical standpoint [1,2]. In the inactive state, a G protein exists as a heterotrimer consisting of an α subunit bound to GDP in association with a βγ complex. Activation of the G protein heterotrimer occurs in a catalytic manner and requires its interaction with an agonist-activated membrane-bound heptahelical receptor. The interactions between the G protein and its complementary receptor trigger the release of two signaling molecules: a tightly associated dimer of β and γ subunits, and a Mg^{2+}–GTP complex of the α subunit [1,3]. The lifetime of the α subunit as a signal carrier is governed by the rate at which it catalyzes the hydrolysis of GTP, typically in the range of ten to twenty seconds. To understand the structural basis of this unusually slow rate of enzyme-catalyzed GTP hydrolysis, it will be necessary to elucidate the critical structural intermediates along the reaction pathway.

The interaction between the G protein and membrane-bound receptor promotes the dissociation of GDP from the α subunit (Gα). The nucleotide-free state is transient owing to the high intracellular concentration of GTP, which quickly occupies the guanine nucleotide binding pocket. Subsequent conformational changes, induced by GTP binding, result in the liberation of Gα–GTP from βγ and allow activation of downstream effectors. The duration of the signal is determined by the intrinsic rate of α subunit catalyzed GTP hydrolysis, or that stimulated by GTPase activating proteins (GAP). The reassociation of Gα–GDP and βγ restores the G protein to the inactive state. Exploitation of a metastable GTP-bound species as both a timer and carrier of information is also characteristic

of other members of the GTPase superfamily [3,4,5]. Of these, perhaps the most extensively studied has been p21ras; mutations that prolong the half-life of the metastable GTP-bound p21ras are oncogenic [6].

Crystallographic and mutational analyses have provided a wealth of structural and mechanistic information on the conformational changes associated with GTP hydrolysis by signal transducing G proteins, p21ras, elongation factor Tu (EF-Tu) and other members of the GTPase super-family [7–18]. Hydrolysis is postulated to occur via an SN2 in-line attack of the γ-phosphate of GTP by a nearby water molecule [19,20]. The crystal structures of Gα subunits complexed with the transition state analog GDP–AlF_4^- have helped to elucidate this mechanism [18,21]. The X-ray structure of GDP–AlF_4^- bound to $G_{i\alpha1}$ shows a square planar complex (AlF_4^-) octahedrally coordinated to a β-phosphate oxygen and a transaxial water molecule. This analog of the pentacoordinate intermediate is stabilized by two highly conserved residues (Arg178 and Gln204 in $G_{i\alpha1}$); mutations of these residues have been shown to dramatically impair GTP hydrolysis. X-ray crystal structures of $G_{i\alpha1}$ bound to either GDP or to the slowly hydrolyzable GTP analog guanosine 5′-O-3′-thiophosphate (GTPγS) [18,22], indicate that the two residues do not form contacts with either the guanine nucleotide or the putative nucleophilic water molecule. However, in the $G_{i\alpha1}$–GDP–AlF_4^- complex [18,21], the Arg178 side chain contacts equatorial fluoride atoms and the βγ-phosphate bridging oxygen [21], while the Gln204 side chain is hydrogen bonded to both the axial water and a fluoride substituent. Based on these observations, it was proposed that the arginine and glutamine residues each play a role in catalysis. The arginine is thought to stabilize the developing charge on the γ-phosphate, whilst the glutamine polarizes and orients the nucleophilic water molecule [18].

Further studies of the stereochemical mechanism of GTP hydrolysis have led to investigations of a mutant of $G_{i\alpha1}$ in which the glycine residue at position 203, conserved in all members of the G protein superfamily, is replaced by an alanine. The functional consequences of this mutation have been well characterized in the corresponding Gly226→Ala mutant of $G_{s\alpha}$, the activator of adenylyl cyclase [23]. This mutant, termed $G226AG_{s\alpha}$, was originally identified in an S49 mouse lymphoma cell line that lacked stimulable adenylyl cyclase activity when challenged with agents that act through G_s [24,25]. The GDP-bound species of $G226AG_{s\alpha}$ was shown to bind βγ with higher affinity than its wild type counterpart. In addition, $G226AG_{s\alpha}$ is incapable of undergoing the conformational changes necessary for GTP-induced dissociation of the α subunit from βγ [26,27]. Further studies, with a recombinant form of the enzyme, demonstrated that the Gly226→Ala mutation results in a 300-fold increase in the estimated K_d for Mg^{2+} ion, thereby impeding formation of the GTP–Mg^{2+} complex. Nevertheless, the affinity of $G226AG_{s\alpha}$ for GDP and k_{cat} is similar to that of the wild type. When reconstituted with adenylyl cyclase, $G226AG_{s\alpha}$ is capable of stimulating cyclase activity and binds with an affinity similar to that of the wild-type protein [27].

Recently, we demonstrated that the conformation of the Gly203→Ala mutant of $G_{i\alpha1}$ ($G203AG_{i\alpha1}$) bound to GDP is essentially identical to that of the wild type GDP complex [22]. It thus appears that the Gly203→Ala mutation affects a conformational step that precedes formation of the GDP (product) complex. Accordingly, we anticipated that the structure of $G203AG_{i\alpha1}$ in the presence of GTPγS [28] would reveal the nature of this conformational perturbation. We describe here the catalytic properties of $G203AG_{i\alpha1}$, and the structure of the subunit crystallized in the presence of GTPγS. The X-ray crystal structure shows that the so-called 'Switch II' region of $G203AG_{i\alpha1}$ adopts a conformation distinct from those seen for the GDP- and GTP-bound forms of $G_{i\alpha1}$. Most remarkably, however, the α subunit is bound to GDP–Pi instead of the expected GTPγS–Mg^{2+}, and thus appears to correspond to a ternary product complex of GTP hydrolysis.

Results and discussion

Catalytic properties of the Gly203→Ala mutant

In many respects $G203AG_{i\alpha1}$ resembles its homolog, $G226AG_{s\alpha}$. For comparison, the catalytic constants of wild type $G_{i\alpha1}$ are given in parentheses, followed by the corresponding constants for $G226AG_{s\alpha}$ and wild type $G_{s\alpha}$, respectively [27,29]. At 10 mM Mg^{2+}, the $G203AG_{i\alpha1}$ k_{cat} for GTP hydrolysis (Fig. 1a) is 2.4 min^{-1} ($G_{i\alpha1}$=4.5, $G226AG_{s\alpha}$=1.5, $G_{s\alpha}$=4.1). Therefore, the mutation has little effect on the intrinsic rate of hydrolysis. The Gly203→Ala mutation also has little effect on the rate of dissociation of GDP (Fig. 1b) as assayed by the 'on' rate for GTPγS (see Materials and methods section). For ($G203AG_{i\alpha1}$) k_{on} for GTPγS = 0.043 ($G_{i\alpha1}$ = 0.029, $G226AG_{s\alpha}$ = 0.19, $G_{s\alpha}$ = 0.17). As in $G_{s\alpha}$, the Gly203→Ala mutation in $G_{i\alpha1}$ lowers the affinity of the subunit for GTPγS in the presence of Mg^{2+} (Fig. 1c; k_{off} = 0.019 min^{-1}); the 'off' rate is too slow to measure for either wild type subunit (the k_{off} for GTPγS is 0.03 min^{-1} for $G226AG_{s\alpha}$). Similarly, the Gly203→Ala mutation only slightly increases the steady-state rate (k_{ss}) of GTP hydrolysis (Fig. 1d; k_{ss} = 0.045 pmol Pi/pmol $G_{i\alpha1}$ min^{-1}), which is dominated by the rate of GDP dissociation ($G_{i\alpha1}$=0.026, $G226AG_{s\alpha}$=0.14, $G_{s\alpha}$=0.15). Although the Gly226→Ala mutation drastically reduces the affinity of $G_{s\alpha}$ for Mg^{2+} ion, the corresponding mutation has a more modest effect on $G_{i\alpha1}$, (Fig. 1e; K_d = 50 nM) ($G_{i\alpha1}$ = 8, $G226AG_{s\alpha}$ = 3000, $G_{s\alpha}$ = 30). Similarly, the Gly203→Ala mutation is less destabilizing to the tertiary structure of $G_{i\alpha1}$, as it does not abolish GTP-dependent tryptophan fluorescence [30], as does the Gly226→Ala mutation in $G_{s\alpha}$ [27] (Fig. 1e). Nevertheless, $G203AG_{i\alpha1}$ is not resistant to

Figure 1

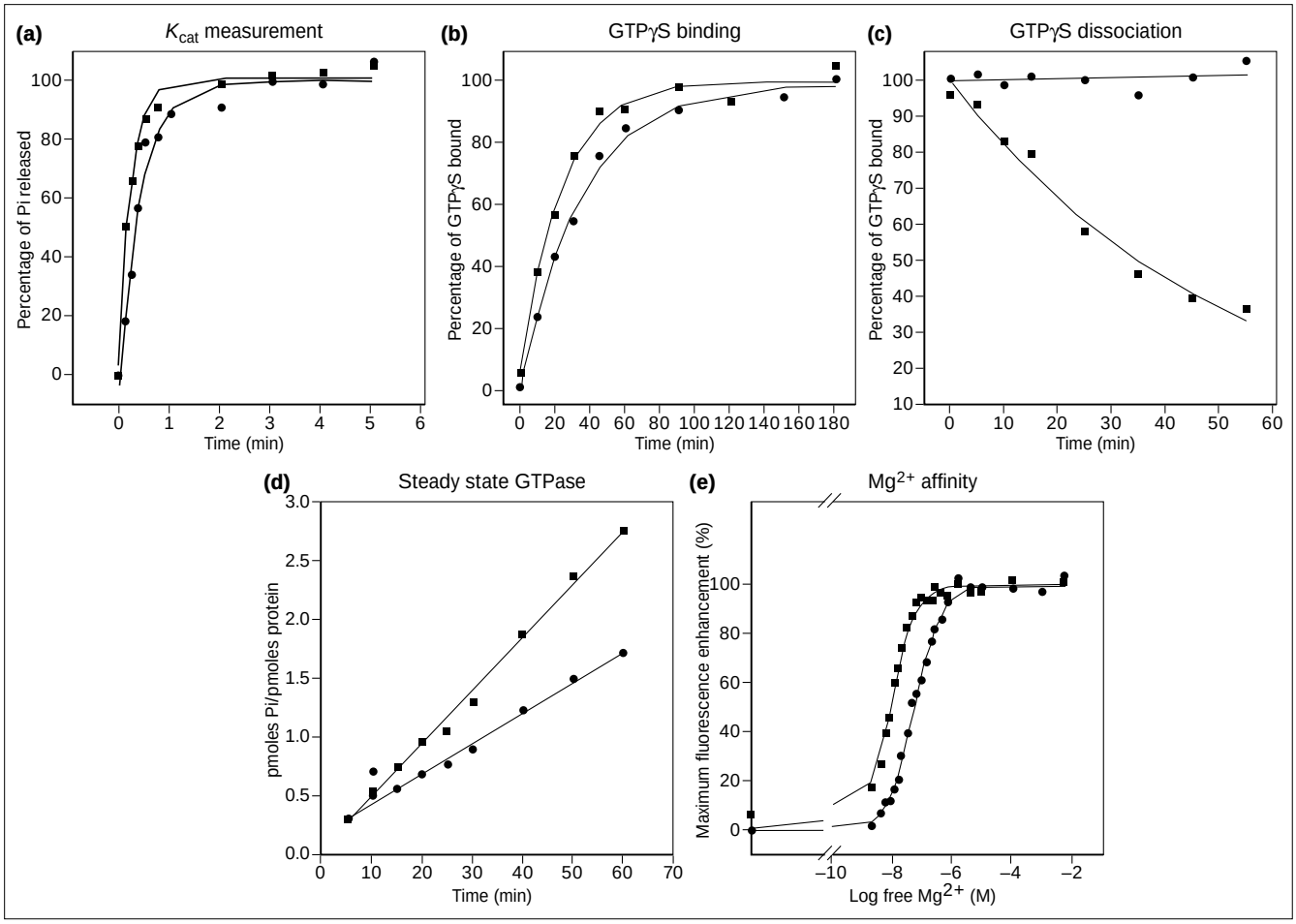

The kinetic properties of G203AG$_{i\alpha1}$ (see Discussion and Materials and methods sections for detailed explanations). Wild type values are plotted with black dots: values for the mutant G203AG$_{i\alpha1}$ are plotted with black squares (**a**) k_{cat} measurement (wild type = 4.5 ± 0.5 min^{-1}, G203AG$_{i\alpha1}$ = 2.4 ± 0.3 min^{-1}); (**b**) GTPγS binding (wild type k_{on} = 0.029 ± 0.02 min^{-1}, G203AG$_{i\alpha1}$ k_{on} = 0.043 ± 0.04 min^{-1}); (**c**) GTPγS dissociation (G203AG$_{i\alpha1}$ k_{off} = 0.019 ± 0.002); (**d**) steady-state GTPase (wild type = 0.026 ± 0.002, G203AG$_{i\alpha1}$ = 0.045 ± 0.003 pmol Pi [pmol protein min]$^{-1}$); (**e**) Mg^{2+} affinity (wild type apparent affinity = 8 ± 1 mM, 203AG$_{i\alpha1}$ = 50 ± 4 mM.

trypsin digestion in the Mg^{2+}, GTP-bound state (ASR *et al.*, unpublished data) as is the wild-type complex of G$_{i\alpha1}$ and other Gα subunits [31].

In summary, it appears that the Gly203→Ala mutation does not perturb the structure or catalytic properties, particularly the Mg^{2+}-binding site, of G$_{i\alpha1}$ to the extent that the corresponding mutation does in G$_{s\alpha}$. Nevertheless, the phenotype originally observed in G$_{s\alpha}$ (i.e. the impaired release of βγ subunits on activation) is preserved, at least qualitatively, in G203AG$_{i\alpha1}$ [32].

Overall structure of G203AG$_{i\alpha1}$

The G203AG$_{i\alpha1}$ mutant appears to be the first member of the G protein superfamily (including the Ras, EF-Tu and elongation factor G [EF-G] families) in which it has been possible to trap the ternary product complex with GDP and Pi (Fig. 2a). In overall structure, as measured by root mean square (rms) differences between corresponding Cα atom positions, the conformation of GDP–Pi-bound G203AG$_{i\alpha1}$ most closely resembles that of the active, GTPγS–Mg^{2+}-bound form (Fig. 2b). Residues 1–33 and 344–354 (the N and C termini) of G203AG$_{i\alpha1}$ are disordered, as in the crystal structure of the wild-type protein in the active state [18]. In crystals of G$_{i\alpha}$–GDP [22], the N and C termini form an ordered microdomain that makes quaternary contacts with the helical domain of an adjacent molecule in the lattice. Because the N terminus is disordered in the structure of G203AG$_{i\alpha1}$–GDP–Pi, these quaternary interactions are not observed. Residues 111–119 in the α-helical domain, termed the Switch IV region (Fig. 2a), participate in G$_{i\alpha1}$ homopolymer interactions

Figure 2

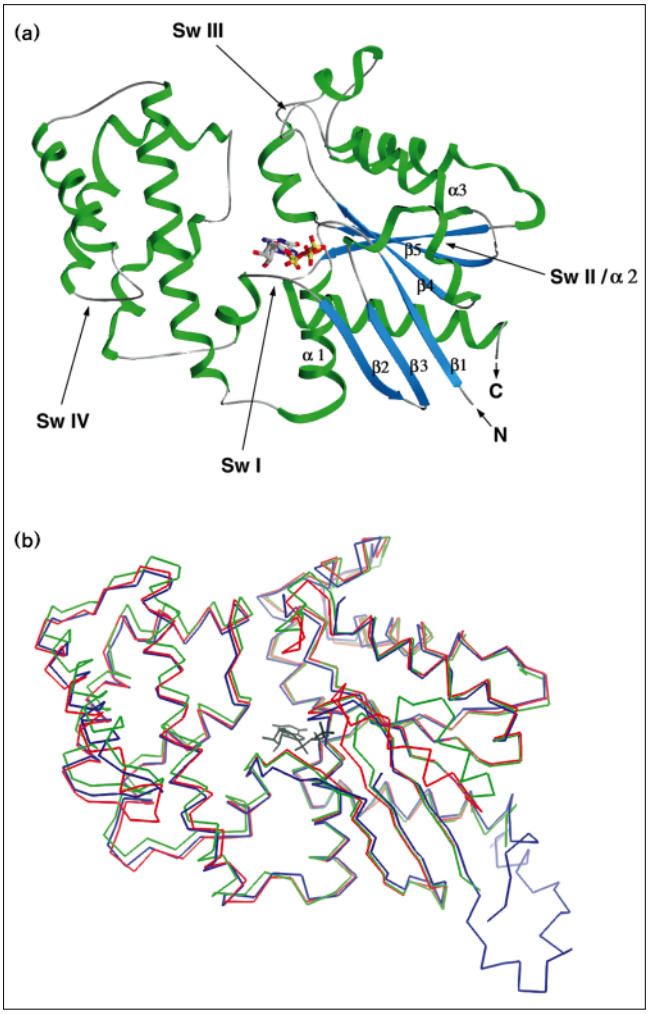

Molecular architecture of G203AG$_{i\alpha1}$. (a) Helical segments are shown as green ribbons and β strands as blue arrows; secondary structural elements near the catalytic site are labeled, GDP and Pi are shown as ball-and-stick models. Switch regions (Sw) are labeled (I–IV) and 'N' and 'C' mark the locations of residues 34 and 343, respectively. (b) A superposition of the Cα traces of the G$_{i\alpha1}$ subunit bound to GDP (blue), G$_{i\alpha1}$ bound to GTPγS–Mg^{2+} (red), and the GDP–Pi complex of G203AG$_{i\alpha1}$ (green). The Cα atoms of residues 40–178 and 220–340 were used to generate the superposition. (Figure was generated using the program SETOR [55].)

in crystals of the GDP complex. The conformation of this region is similar to that of the GDP-bound state rather than that of the GTPγS–Mg^{2+}-bound conformation, even though homopolymer interactions are not observed. The conformation of residues 177–187 (the Switch I region) more closely resembles the GTP-bound state, whereas residues 231–242 (the switch III region), although ordered, are pulled away from the catalytic site. As described below, the conformation of residues 199–219 (Switch II helix) is entirely novel. In essence, the conformation of G203AG$_{i\alpha1}$–GDP–Pi is intermediate between that of the active (GTP-bound) and inactive (GDP-bound) forms. This observation suggests that this complex may be similar to a state assumed by the wild-type protein after cleavage of the γ–phosphate, but prior to the release of the phosphate ion.

Nucleotide-binding site

Although crystals of G203AG$_{i\alpha1}$ were grown in the presence of GTPγS, the catalytic site is occupied by a GDP molecule and a tetrahedral ion; the electron density was modeled as a phosphate ion derived from the crystallization buffer (Fig. 3a). Presumably the GDP molecule arose as either a product of acid-catalyzed (pH = 5.5–5.8) or enzyme-catalyzed hydrolysis of GTPγS, alternatively it may have been present as a contaminant. Subsequent experiments demonstrated that identical crystals can be obtained under the same crystallization conditions with GDP substituted for GTPγS. Conversely, we have not been able to grow crystals of the G203AG$_{i\alpha1}$–GTPγS–Mg^{2+} complex under conditions that have proven successful with wild type G$_{i\alpha1}$ subunits [28].

The non-covalent contacts observed between G203AG$_{i\alpha1}$ and the nucleoside monophosphate moiety of GDP are similar to those observed in all of the other G$_{i\alpha1}$ complexes we have studied [18,22,33] (Fig. 3b). Contacts between the phosphate-binding loop (P loop) (residues 40–44 connecting the β1 strand to the α1 helix) and the α- and β-phosphates of GDP are identical to those observed in the other structures. In contrast, the enzyme employs a different strategy to bind the β- and γ-phosphates which, in this complex, are not in covalent contact. Lys180 in the Switch I region, which is disordered in the G$_{i\alpha1}$–GTPγS–Mg^{2+} complex, is hydrogen bonded to Pi. The well ordered guanidinium moiety of Arg178 donates a hydrogen bond to one oxygen substituent each of the β-and γ-phosphates. Arg178 is poorly ordered in the G$_{i\alpha1}$–GTPγS–Mg^{2+} complex and does not contact the phosphate groups, whereas in the G$_{i\alpha1}$–GDP–Mg^{2+}AlF$_4^-$ complex it is a well ordered ligand of the β-phosphate and fluoride substituents. In the GDP complex, Arg178 bridges the α- and β-phosphates but is characterized by high thermal parameters. In addition, there is a hydrogen bond between Pi and the β-phosphate of GDP (Fig. 3a).

From the structure of G203AG$_{i\alpha1}$ we infer that the interaction between the γ-phosphate and the N terminus of the Switch II helix is maintained throughout the process of β–γ bond cleavage. In both the G$_{i\alpha1}$–GTPγS–Mg^{2+} and the G203AG$_{i\alpha1}$–GDP–Pi complexes, the amide nitrogen of residue 203 donates a hydrogen bond to an oxygen atom of the γ-phosphate (Fig. 3). This hydrogen bond persists even as the γ-phosphate is translated by ~1.5 Å concomitant with bond cleavage. A substantial conformational change in the Switch II helix, promoted by the Gly203→Ala mutation, preserves this interaction.

Figure 3

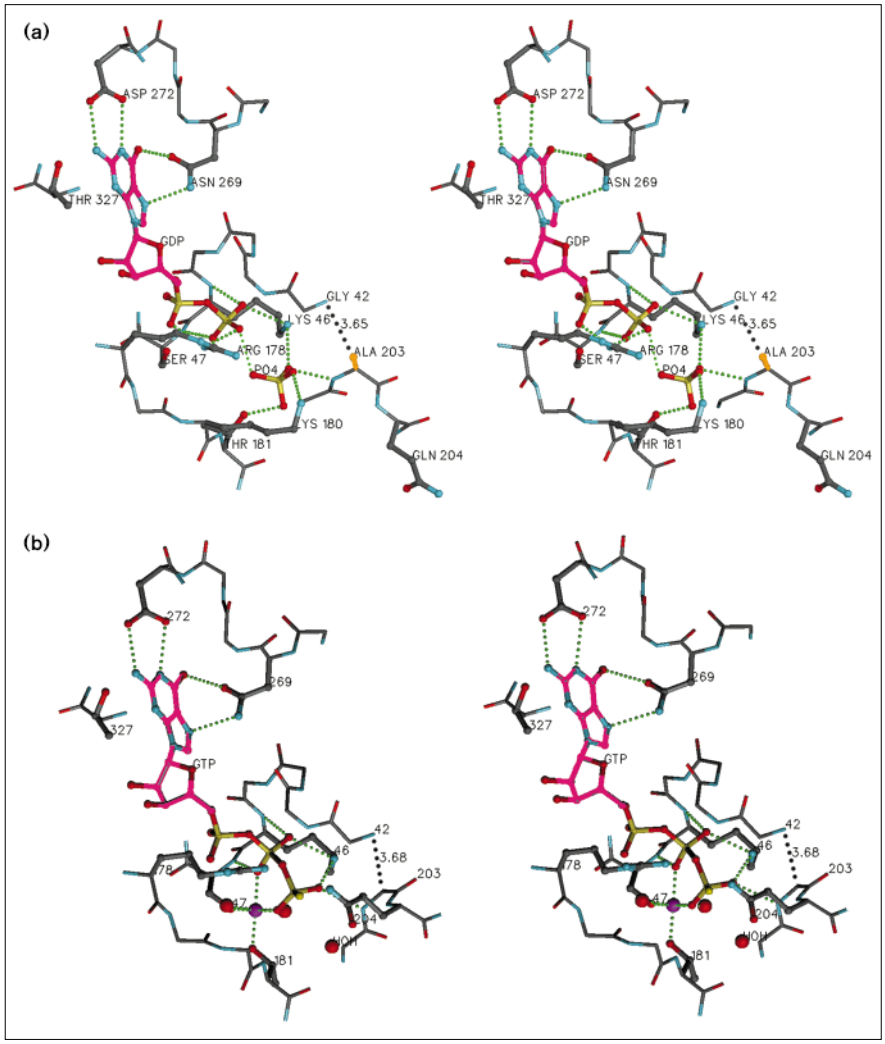

Views of the catalytic site. (a) The G203AG$_{i\alpha1}$–GDP–Pi complex. The main-chain and side-chain skeleton is shown with thin and thick bonds, respectively. Atoms are colored as follows: nitrogen, cyan; carbon, gray; oxygen, red; sulfur, yellow. Carbon atoms in the nucleotide are colored pink and Ala203 is highlighted in orange. Selected hydrogen bonds are shown as green dots; the contact between residues 42 and 203 is shown with gray dots. (b) The Gi$_{\alpha1}$–GTPγS–Mg^{2+} complex. The Mg^{2+} ion is shown as a magenta sphere, and selected water molecules bound at the active site are shown as red spheres. (Figure was generated using the program SETOR [55].)

Loss of the Mg^{2+}-binding site

The conformation of the Switch I region, which supports the Mg^{2+}-binding site, is similar to that observed in the G$_{i\alpha1}$–GTPγS–Mg^{2+} complex, but it is shifted by approximately 1 Å away from the nucleotide. Even though Mg^{2+} is present in the crystallization medium (5 mM), the divalent cation is not visible in the catalytic site. The side chain of one of the metal ligands, Thr181, rotates 90° to allow formation of a hydrogen bond with Pi, as noted above. Thus, the binding site for the Mg^{2+} is partly dismantled before the phosphate leaving group dissociates from the enzyme. No Mg^{2+} is present in the G$_{i\alpha1}$-GDP complex [22].

Rearrangement of the Switch II helix

Model building demonstrates that substitution of an alanine side chain at position 203 results in steric conflict between the β-methyl group and main-chain atoms of Gly42 in the GTP-bound conformation of the subunit. Therefore, conformational differences between the wild type and G203AG$_{i\alpha1}$ are expected, even though the backbone conformation of Gly203 falls within the allowed region for non-glycine side chains (Fig. 4). The conformational differences that result from the Gly→Ala mutation avoid this potential steric conflict and create a binding subsite for the γ-phosphate leaving group. In essence, the α2 helix is extended in the N-terminal direction by half a turn, while a 60° kink is introduced at residue Arg208 (Fig. 5). The rearrangement of Switch II is achieved by discrete changes in the ϕ and ψ angles (Fig. 4), particularly at residues Val201–Gln204, Arg208 and Glu216–Val217. The conformation of G$_{i\alpha1}$–GTPγS–Mg^{2+} is roughly extended from Phe199 to Gly203 and forms a continuous helix between residues Arg205 and Cys214. In contrast G203AG$_{i\alpha1}$ forms two helical segments, Ala203 to Glu207 and Lys209 to Phe215. The latter segment rotates by 180° (Fig. 6), such that Trp211 is transferred from the interface with helix α3 to a more exposed site on the opposite side of the helix axis. In the presence of Mg^{2+} and GTPγS,

Figure 4

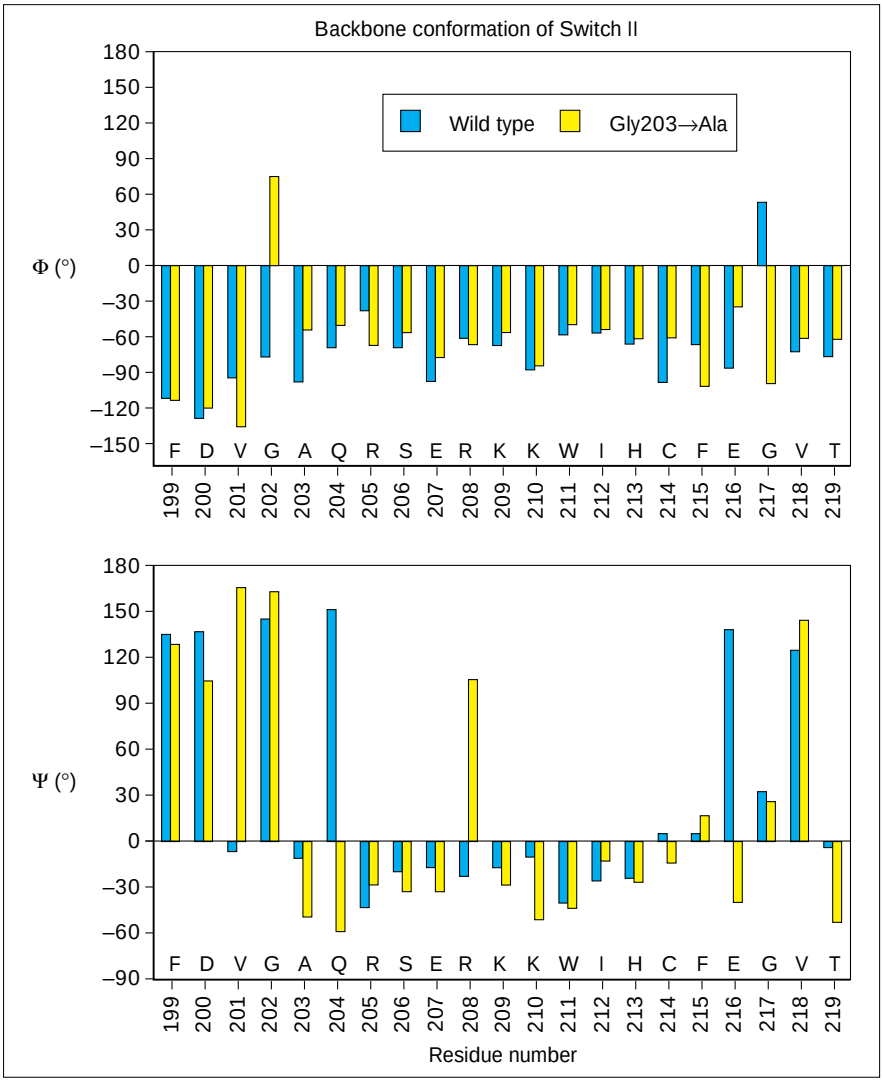

Histogram comparing the main chain ϕ and ψ torsion angles in Switch II. Values for the wild type $G_{i\alpha1}$–GTPγS–Mg^{2+} complex are shown in blue and for $G203AG_{i\alpha1}$–GDP–Pi are shown in yellow.

$G203AG_{i\alpha1}$ exhibits the strong tryptophan fluorescence characteristic of the activated wild-type protein (Fig. 1e). However, spectra have not been measured of the protein in the GDP–Pi state. The kink at Arg208 (Fig. 5a) directs the helical dipole of the first helical segment toward the free phosphate ion in the active site. Exposure of the polypeptide chain at the kink site may account for the susceptibility of $G203AG_{i\alpha1}$ to trypsinolysis in the GTPγS–Mg^{2+}-bound conformation (ASR *et al.*, unpublished data). The mutant and wild-type structures also differ by a 180° flip in the orientation of the Glu216 peptide plane (not shown); the following glycine residue (Gly217) consequently switches from an α_L to a γ_R conformation (in the nomenclature of Wilmot and Thornton [34]).

The Switch II segments in GTPγS–Mg^{2+}-bound wild type $G_{i\alpha1}$ and the $G203AG_{i\alpha1}$–GDP–Pi complex adopt not only alternative secondary structures but also different packing arrangements within the tertiary structure of the enzyme. The two conformations for Switch II are both supported by numerous interactions with the protein, as detailed in the following discussion. In $G_{i\alpha1}$ (Fig. 6b), Switch II is packed against the hydrophobic surfaces of the α3 helix and between the β1 and β3 strands. In the mutant (Fig. 6a), Switch II kinks toward α3 and shifts about 5 Å to settle on a hydrophobic-binding platform, directly over the β1 strand. Virtually every residue in Switch II occupies a different neighborhood in the two structures. However, with few exceptions, the type of environment occupied by each residue is preserved. Thus, the six charged residues in Switch II are solvent exposed in both structures, although certain specific electrostatic contacts present in $G_{i\alpha1}$ are not found in the mutant. In $G203AG_{i\alpha1}$ the ionic interactions (Fig. 6b) of Glu236 and Glu245 in the Switch III loop,

Figure 5

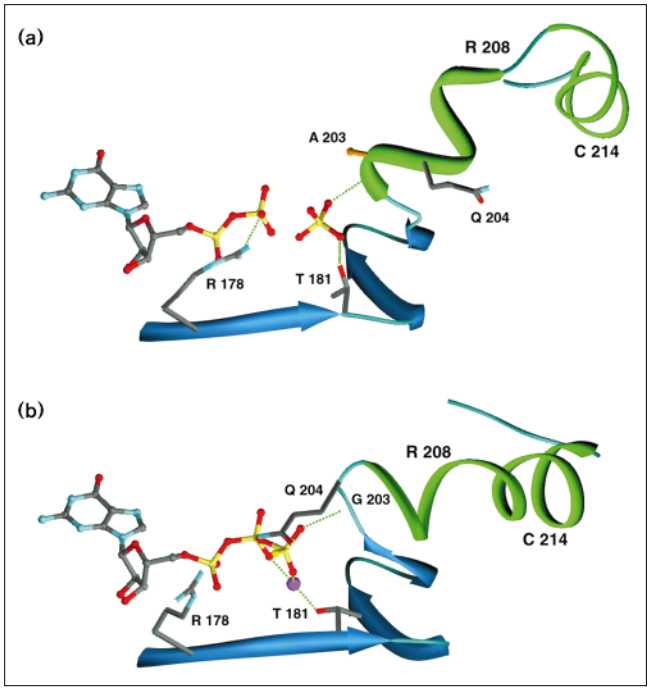

Ribbon and arrow model of the Switch I–β2–β3–Switch II (α2) region in two complexes: (a) G203AG$_{i\alpha1}$–GDP–Pi and (b) G$_{i\alpha1}$–GTPγS–Mg^{2+}. Helices are shown in green and β strands in blue; the atom coloring scheme is as described in Figure 3. (Figure was generated using the program SETOR [55].)

Figure 6

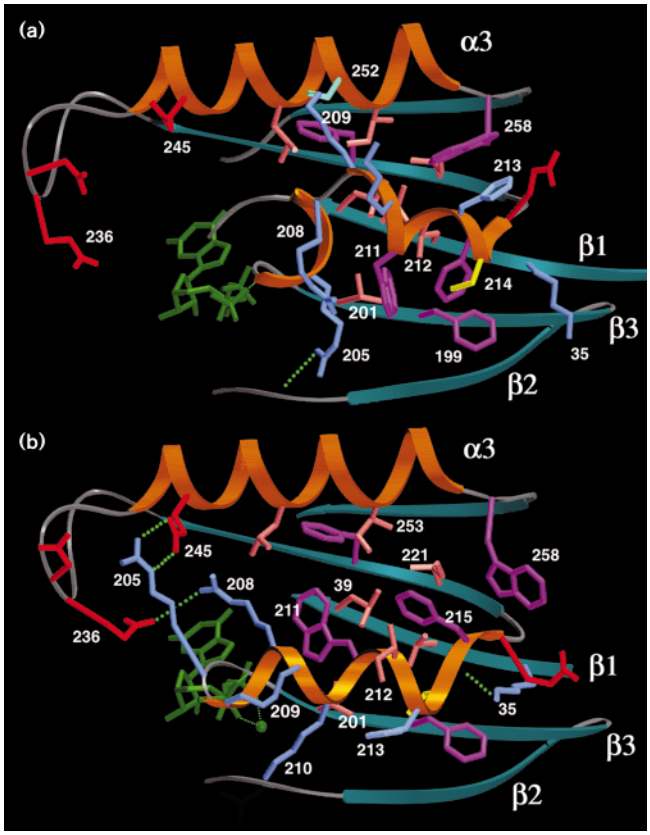

Packing surface of the Switch II helix in (a) G203AG$_{i\alpha1}$–GDP–Pi and (b) G$_{i\alpha1}$–GTPγS–Mg^{2+} complexes. Helices are shown in orange and β strands in blue. Side chains are colored blue for lysine, arginine and serine; red for glutamate and aspartate; magenta for phenylalanine and tryptophan and pink for valine, leucine and isoleucine. The guanine nucleotide is colored green. (see text for details). (Figure was generated using the program SETOR [55].)

with Arg205 and Arg208 in α2 are lost (Fig. 6a), with the concomitant displacement of Switch III away from the Switch II helix. Similarly, the 'capping' interaction between Lys35 in the β1 strand and the carbonyl oxygen atoms of Cys214 and Glu216, at the C terminus of the α2 helix (Fig. 6b), is absent in the mutant. In partial compensation (Fig. 6a), Arg205 and Lys209 form hydrogen bonds with the carbonyl oxygen of Thr182 and the hydroxyl group of Ser252, respectively.

More of the hydrophobic residues in Switch II are buried in G203AG$_{i\alpha1}$. Ile212, in particular, is completely exposed in the wild-type subunit (Fig. 6b), but is transferred to a buried site above the β1 strand in the G203AG$_{i\alpha1}$ complex (Fig. 6a). Although Trp211 is not bound at a protein–protein interface in G203AG$_{i\alpha1}$, it is partly enveloped in a hydrophobic microenvironment comprising Val201, Phe215 and Cys214. The imidazole side chain of His213 is stacked over the indole ring of Trp258 in the mutant (Fig. 6a) but is completely solvent accessible in the wild-type subunit (Fig. 6b). In both structures (Fig. 3), the van der Waals contact between residue 203 and the peptide plane of Gly42 is maintained; the position occupied by the β-methyl group of Ala203 is nearly identical to that occupied by the hydrogen substituent in Gly203 (Fig. 3).

Implications for activation mechanisms

On comparing the structures of several members of the G protein superfamily, we find that the conformation of the Switch II region in the GTP-bound state is essentially the same in all these molecules. In contrast, the Switch II regions of the GDP-bound proteins adopt a variety of conformations (Fig. 7). As others have observed [13], the γ-phosphate moiety of GTP anchors the N terminus of Switch II. In its absence, an essential constraint is lost, and Switch II is free to adopt a variety of conformations. Switch II in G$_{i\alpha1}$ is a malleable structure, adopting a different conformation in each of its GDP-bound states. The succession of positively charged and bulky residues in the primary sequence may confer an intrinsic instability to the α2 helix. Alternative conformations adopted in the series of nucleotide complexes described here may be stabilized by a few favorable interactions with the β-phosphate, Pi or G protein βγ subunits. In the GDP complex where the Mg^{2+} and Pi subsites are empty and βγ is absent, Switch

II is completely disordered. Despite the high sequence similarity between $G_{i\alpha1}$ and $G_{t\alpha}$, the Switch II conformation in GDP-bound $G_{t\alpha}$ differs from that in $G_{i\alpha1}$ [17]. This could be attributed to differences in the crystallization conditions, Mg^{2+} ion occupancy, presence or absence of the N terminus, and crystal packing interactions.

The most striking property of $G203AG_{i\alpha1}$ is its inability to dissociate from βγ subunits in the presence of GTP. Structures of heterotrimeric complexes of $G_{i\alpha1}$ [33] and a $G_{i\alpha1}/G_{t\alpha}$ chimera [35] show extensive interaction surfaces between the βγ subunits and the Switch II helix of the α subunit. However, structural studies of the $G203AG_{i\alpha1}$–GDP–βγ complex (MA Wall and SRS, unpublished data) reveal no substantial differences between the Switch II conformations in the mutant and wild type complexes. It is possible that the Gly→Ala mutation stabilizes the conformation of Switch II which is most complementary to the surface of βγ. Indeed, the position and orientation of Switch II in the $G203AG_{i\alpha1}$–GDP–Pi and wild-type $G_{i\alpha1}$–GDP–βγ complexes are roughly similar (Fig. 7). More importantly, the conformational change ordinarily induced by GTP binding would result in steric conflict between the β-methyl group of Ala203 and the peptide bond of Gly42. Thus, dissociation of $G_{i\alpha1}$–GTP from βγ would be inhibited. Because it has not been possible to crystallize the GTPγS–Mg^{2+} complex of $G203AG_{i\alpha1}$, we do not know how the protein relieves strain at the interface between Ala203 and the P loop. Fortunately, the Gly42→Val mutant does crystallize in all three states: GTPγS–Mg^{2+}, GDP–Pi and GDP (ASR *et al.*, unpublished data). The Gly42→Val mutation perturbs the same protein–protein interface as the Gly203→Ala, mutation and therefore analysis of the Gly42→Val $G_{i\alpha1}$ structure should reveal how such accommodation is made in the Michaelis complex.

Figure 7

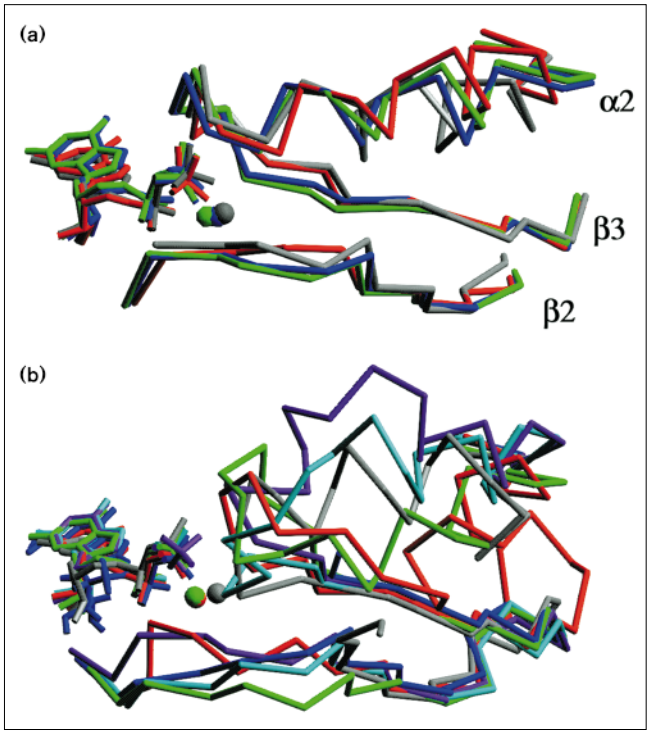

Superposition of the Switch II regions of several G protein superfamily members. (**a**) G proteins in the active GTP- bound state: EF-Tu–GDPNP (gray); $G_{i\alpha1}$–GTPγS (blue); G_t–GTPγS (green); and p21ras– GDPCP (red). (**b**) G proteins in the inactive, GDP-bound state. EF-Tu–GDP (gray); $G_{i\alpha1}$–GDP (dark blue); $G203AG_{i\alpha1}$–GDP–Pi (purple); $G_{i\alpha1}$–GDP–$\beta_1\gamma_2$ (light blue); G_t–GDP (green); and p21ras–GDP (red). Coordinates were taken from the Protein Databank [56] with accession numbers EF-Tu–GDPNP, 1eft; EF-Tu–GDP, 1etu; p21ras–GDPCP, 6q21; p21ras–GDP, 4q21; $G_{t\alpha}$–GTPγS–Mg^{2+}, 1tag; $G_{t\alpha}$–GDP–Mg^{2+}, 1tnd; $G_{i\alpha1}$–GTPγS–Mg^{2+}, 1gia, $G_{i\alpha1}$–GDP, 1gdd. Coordinates for $G_{i\alpha1}$–GDP–$\beta_1\gamma_2$ are taken from Wall *et al.* [33] and are available from the authors by internet. (Figure was generated using the program SETOR [55].)

Implications for the mechanism of catalysis by G protein α subunits

It is our hypothesis that the Gly203→Ala mutation, together with the relatively acidic conditions in which the protein was crystallized, appears to have stabilized an otherwise transient intermediate of $G_{i\alpha1}$-catalyzed GTP hydrolysis. Kinetic studies [36] of $G_{s\alpha}$ have demonstrated that phosphate release is not rate limiting in the hydrolysis of GTP, suggesting that the ternary complex with GDP and phosphate ion is unstable. Crystal structures of both the wild type $G_{i\alpha1}$–GTPγS–Mg^{2+} and $G_{i\alpha1}$–GDP complexes indicate that neither conformation should stabilize a ternary complex. Thus, the structure of the GDP-bound conformation of wild type and $G203AG_{i\alpha1}$ are virtually identical. In both, the Switch II helix is completely disordered, with the concomitant loss of the γ-phosphate binding site. In the active GTPγS–Mg^{2+} complex, the transfer of the γ-phosphate to a site corresponding to that filled by the phosphate ion in $G203AG_{i\alpha1}$–GDP–Pi would result in steric conflict with the N terminus of the Switch II helix. Therefore, formation of the GDP–Pi ternary complex, as observed in the present structure, is contingent upon the rearrangement or repositioning of Switch II. If the ternary complex observed in $G203AG_{i\alpha1}$ indeed mimics that which occurs in the reaction catalyzed by the native enzyme, we might infer that an obligate step in catalysis corresponds to a conformational change in which the Switch II helix is reorganized. Specifically, we suggest that it is the dissociation of the leaving group from the pentacoordinate intermediate of the SN2 reaction that requires this conformational step.

The recently determined structures of several $G_{i\alpha1}$ complexes may now be ordered as a series of 'snap-shots', depicting discrete states along the reaction coordinate of G protein-catalyzed GTP hydrolysis (Fig. 8). In each of the states so far characterized, the nucleoside diphosphate moiety of the guanine nucleotide is held rigidly

Figure 8

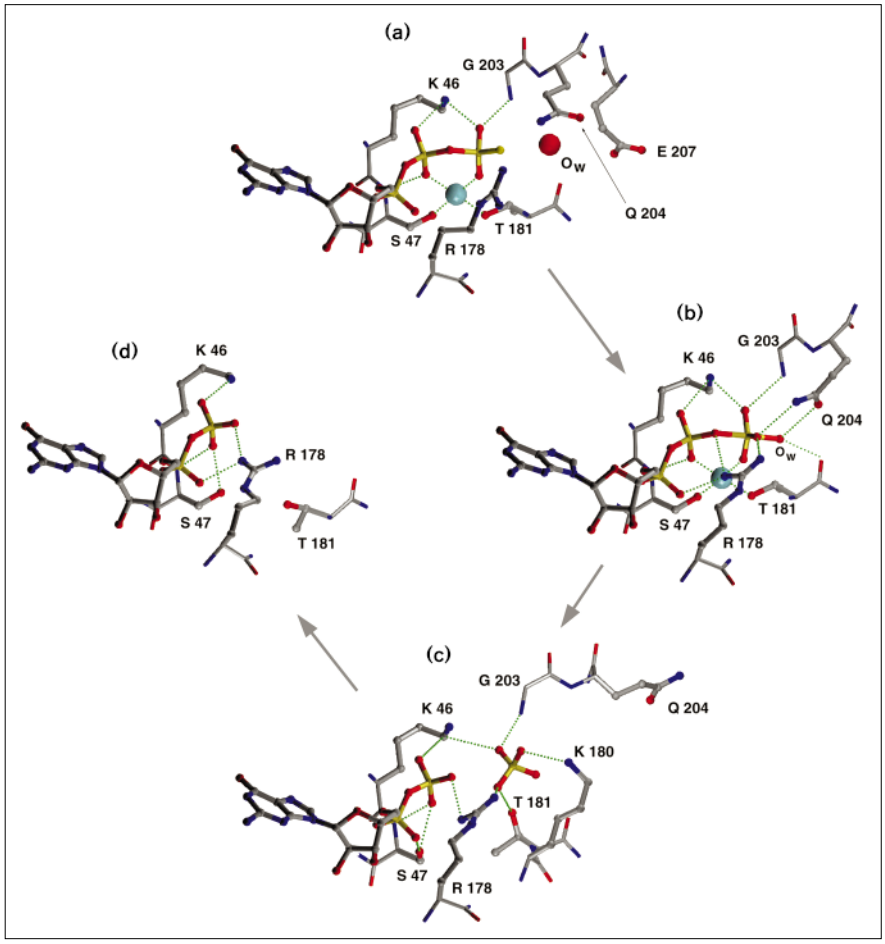

Conformational states along the reaction pathway (see text). (a) $G_{i\alpha1}$–GTPγS–Mg^{2+}. (b) Structure of the pentacoordinate intermediate modeled on the structure of the $G_{i\alpha1}$–GDP–AlF_4^-–Mg^{2+} complex. (c) $G_{i\alpha1}$–GDP–Pi complex modeled on the structure of G203A–GDP–Pi. (d) $G_{i\alpha1}$–GDP. Color scheme is the same as that used in Figure 3. (Figure was generated using the program SETOR [55].)

in the catalytic site; the only conformational changes are associated with structural elements that recognize the γ-phosphate or the Mg^{2+} ion.

The enzyme–substrate complex

The $G_{i\alpha1}$–GTPγS–Mg^{2+} substrate complex (Fig. 8a) is presumed to closely resemble the structure of the $G_{i\alpha1}$–GTPγS–Mg^{2+} complex [18]. The N terminus of the Switch II helix is directed toward the γ-thiophosphate group; both Lys46 and the amide of Gly203 form hydrogen bonds with a thiophosphate oxygen atom. A second γ-phosphate oxygen is a Mg^{2+} ion ligand. The β,γ-phosphate bridging oxygen is hydrogen bonded to the amide nitrogen of Glu43 (not shown). A water molecule, located 3.8 Å from the γ-phosphorous atom and axial to the β,γ-phosphate bridging oxygen, is positioned for a nucleophilic attack. The two catalytic residues, Arg178 (Switch I) and Gln204 (Switch II helix) are poorly ordered and do not contact the substrate.

The pentacoordinate intermediate

The pentacoordinate intermediate (Fig. 8b) is mimicked by the $G_{i\alpha1}$–GDP–AlF_4^-–Mg^{2+} complex [18,21]. Here, the square planar AlF_4^- group forms an octahedral complex in which the β,γ-phosphate bridging oxygen and a water molecule or hydroxylate ion are transaxial ligands. The side chain of Arg178 is well ordered and has rotated to form hydrogen-bond contacts with an α-phosphate oxygen, the β,γ-phosphate bridging oxygen, and a fluoride atom of the square planar AlF_4^- group. The stereochemistry of the pentacoordinate intermediate can be roughly inferred from the structure of the $G_{i\alpha1}$–GDP– AlF_4^-–Mg^{2+} complex. Arg178 could hydrogen bond with the pyramidal oxygen atoms of the γ-phosphate, thus stabilizing charge development expected in an associative transition state. The arginine could also form hydrogen bonds with the β,γ-phosphate bridging oxygen which, together with that to the amide group of Glu43, would stabilize a dissociative transition state [37]. The structure of the $G_{i\alpha1}$–GDP–AlF_4^-–Mg^{2+} is not inconsistent with either mechanism. The Mg^{2+} ion is expected to function as a Lewis acid through its ligand field interaction with a second periplanar oxygen.

Gln204 rotates in the $G_{i\alpha1}$–GDP–AlF_4^-–Mg^{2+} complex to accept a hydrogen bond from the putative water

nucleophile; Gln204 donates a hydrogen bond to a fluoride atom. These interactions, together with hydrogen bonding to the carbonyl oxygen of Thr181, polarize and orient the lone pair orbitals of the attacking water molecule. The hydrogen bond with Thr181 is maintained in both the GTPγS–Mg^{2+} and the GDP–AlF_4^-–Mg^{2+} complexes of $G_{i\alpha1}$. Indeed, with the exception of Gln204 and Arg178, none of the residues in the catalytic site have moved substantially, relative to their position in the $G_{i\alpha1}$–GTP γS–Mg^{2+} complex.

The GDP–Pi ternary complex

The GDP–Pi ternary complex (Fig. 8c) may resemble the G203A$G_{i\alpha1}$–GDP–Pi complex. As described above, the Gly→Ala mutation is expected to introduce steric strain, therefore, it is probable that the ground state conformation differs somewhat from that in the native enzyme. The Switch I segment moves slightly away from the catalytic site, such that the Mg^{2+} ion is no longer tightly bound. However, in the native complex the Mg^{2+} ion may still be resident at the active site. Arg178 reorients only slightly, forming hydrogen bonds with both the β-phosphate and the phosphate ion. Lys180 and Thr181 (formerly a Mg^{2+} ligand) also reorient to form hydrogen bonds with the leaving group. The massive restructuring of the Switch II helix results in the dissolution of ionic contacts with Switch III. The increased disorder in this segment may be due to loss of these contacts. Most notably, the conformational rearrangement of Switch II transfers Gln204 out of the catalytic site, guides the dissociation of the bipyramial pentacoordinate intermediate, and creates a transient phosphate-binding site. At neutral pH, this state is expected to be unstable due to the negative charge originating from GDP (–3) and Pi (–2).

The binary GDP complex

With the dissociation of product phosphate from the enzyme active site, the Switch II segment from residues 200–218 becomes completely disordered (Fig. 8d). The Switch I segment shifts further from the nucleotide. Conformational changes in this region are centered on Lys180, which, upon dissociation of the phosphate ligand, rotates out of the active site, as does the Mg^{+2} ligand, Thr181. Arg178 is only loosely associated (judging from weak side chain electron density) with the α- and β-phosphate groups of GDP. Thus the catalytic apparatus is largely dismantled in the binary complex. In the $G_{i\alpha1}$–GDP complex, the N and C termini are assembled into a small folding domain. The implications of this refolding event are discussed elsewhere [22].

Further structural studies [33,35] have shown that the Switch II helix again reorders upon association of $G_{i\alpha1}$–GDP with the βγ complex. In this state, Switch II adopts a conformation that is markedly different from that observed in either the GTP-bound or GDP–Pi conformations. Coupled main-chain displacements of Switches I and II lock GDP into the catalytic site, partly through the formation of an ion-pair–hydrogen bond contact between Glu43 and Arg178. The conformation of Switch II in the GDP–Pi complex appears to be intermediate between that of the GTPγS-activated protein and heterotrimeric $G_{i\alpha1}$–GDP.

Rate enhancement of the GTPase reaction catalyzed by Ras and G protein α subunits is due primarily to transition state stabilization [18,38,39]. For Ras, NMR spectroscopic data, pH activity profiles and a Brønsted analysis point to a general base with a p*K*a near to 3 [40]. This observation suggests, along with theoretical studies [39], that the γ-phosphate of GTP itself extracts a proton from the attacking water molecule. In the structure of $G_{i\alpha1}$–GTPγS–Mg^{2+}, only two of the three γ-phosphate oxygen atoms participate in a hydrogen bond with the enzyme. A third phosphate oxygen atom, located 3.3 Å away from the presumptive water nucleophile, is thus available for proton extraction. Formation of the pentacoordinate intermediate requires, at the least, the orientation of two side chains. Dissociation of this complex may be limited by the rate at which the nucleophile is deprotonated, but also appears to require rearrangement of the Switch II helix. It is possible, as discussed above, that the collapse of the pentacoordinate intermediate to products may correspond to the rate limiting step of the reaction.

Proteins (GAPs) that stimulate the GTPase activity of Ras may function in part as co-enzymes, supplying a catalytic residue to the catalytic apparatus and thereby stabilizing the pentacoordinate intermediate [41]. For example, a single arginine residue in the GAP domain of neurofibromin is deemed critical to Ras activation [41,42], in a role analogous to that of Arg178 [41,43]. Regulators of G protein signalling (RGS) have been recently shown to accelerate GTP hydrolysis by α subunits of the G_i family [44], has much greater affinity for the AlF_4^-–GDP-bound form of the protein (transition state mimic) than for either the GTPγS- or GDP-bound subunits [45]. However, the powerful rate enhancement provided by GAP proteins suggests that they accelerate both the formation of the reaction intermediate and the conformational changes that may be required for its breakdown to products.

Biological implications

Upon the hydrolysis of GTP, the **α** subunits of G proteins undergo a conformational transition that causes them to dissociate from effector molecules and reassociate with inhibitory **βγ** subunits. The structure of a G protein **α** subunit, $G_{i\alpha1}$, complexed with a slowly hydrolyzable analog of GTP (GTP**γ**S) and the structures of both the free and **βγ**-bound forms of $G_{i\alpha1}$–GDP demonstrate that this conformational transition is centered on a region of the protein called the Switch II helix. The Switch II helix

forms the γ-phosphate recognition site, part of the catalytic apparatus, and interacts with both effectors and βγ subunits. GTP hydrolysis, which is characterized by an unusually weak rate enhancement for an enzyme-catalyzed reaction (the single turnover rate is 2–5 min^{-1}), is directly coupled to a conformational transition. Here, we describe the structure of a mutant of $G_{i\alpha1}$ in which the glycine residue at position 203 (at the N terminus of the Switch II helix) is replaced by an alanine residue. This mutant has a reduced affinity for the Mg^{2+} required for catalysis, and fails to release βγ subunits upon binding GTP. Nevertheless, the single turnover rate for catalysis is similar to that of the wild-type enzyme.

We have crystallized a ternary complex of G203A$G_{i\alpha1}$ with GDP and inorganic phosphate; the structure of this complex has provided an unexpected view of a putative catalytic intermediate. The Gly203→Ala substitution would, in the native enzyme, result in steric conflict between the Switch II helix and the phosphate-binding loop (residues 40–44). In the mutant, this conflict is avoided by a rearrangement of the Switch II region which, simultaneously, creates a binding site for the leaving group phosphate. We propose that the Gly203→Ala mutation, at low pH (< 5.8), stabilizes a conformation similar to the normally transient ternary complex. If this is correct, it follows that a conformational transition accompanies the dissociation of the pentacoordinate intermediate. The requirement for such a transition might account for the unusually low single turnover rate of GTP hydrolysis in $G_{i\alpha1}$ in particular, and possibly for other members of the Ras superfamily.

The high activation barrier of enzyme-catalyzed GTP hydrolysis ensures that the lifetime of the active Gα–GTP complex is sufficient to achieve the necessary level of signal amplification. The structural data presented here suggest that a specific linkage between catalysis and backbone conformational changes provides a relaxation mechanism for appropriate decay of the Gα–GTP signal. Protein cofactors that accelerate the rate of G protein catalyzed GTP hydrolysis (e.g. GTPase activating proteins) could function by reducing the activation energy barrier of such a conformational transition along the reaction coordinate.

Materials and methods

Protein preparation

Recombinant $G_{i\alpha1}$ and G203A$G_{i\alpha1}$ proteins were obtained by expression in *Escherichia coli* BL21(DE3) cells, using an isopropyl-1-thio-D-galactopyranoside (IPTG) inducible pQE-6 vector, as previously described [28,46]. Purified proteins were exchanged into $H_{50}E_1D_5$ (50 mM N-(2-hydroxyethyl) piperazine-N^L(2-ethanesulfonic acid (HEPES) pH 7.0), 1 mM ethylenediaminetetraacetic acid (EDTA), and 5 mM dithiotheritol (DTT) containing 50 μM GDP by sequential dilution and concentration in a Centricon PM30 (Amicon). Purified proteins were concentrated to 10–20 mg ml^{-1}, snap frozen in liquid nitrogen, and stored at –80° C.

GTPγS binding kinetics

$G_{i\alpha1}$ proteins (200 nM) were incubated at 30° C in 50 mM NaHEPES (pH 8.0), 1 mM EDTA, 5 mM DTT, 0.05 % Lubrol, 10 mM $MgSO_4$ and 1 μM [^{35}S]GTPγS (3000 cpm pmole^{-1}). Aliquots (100 μl) were withdrawn at the indicated time intervals, added to wash buffer at 0°C (20 mM Tris·HCl pH 8.0, 100 mM NaCl and 25 mM $MgCl_2$) and applied to BA-85 (Schleicher and Schuell 0.45 μm) filters, whereupon the radioactivity was quantified [47]. Values of k_{app} were calculated by a nonlinear least-squares fit to $B = B_{eq}(1–e^{–kt})$.

GTPγS dissociation kinetics

$G_{i\alpha1}$ proteins (200 nM) were incubated for 90 min with 1 μM [^{35}S]GTPγS as described above. GTP was then added to a final concentration of 200 μM. Aliquots (80 μl) were withdrawn at the indicated time intervals and counted as previously described above. Values of k_{app} were calculated by a nonlinear least-squares fit to $B = B_o e^{–kt}$.

Steady-state hydrolysis of GTP

$G_{i\alpha1}$ proteins (200 nM) were incubated at 30° C in 50 mM NaHEPES (pH 8.0), 1 mM EDTA, 5 mM DTT, 0.05 % Lubrol, 10 mM $MgSO_4$, and 1.5 μM [γ-^{32}P]GTP (3000 cpm pmole^{-1}). At the indicated time intervals, aliquots (50 μl) were withdrawn, added to 750 μl of 5 % (w/v) Norit in 50 mM NaH_2PO_4 (0° C) and vortexed. The charcoal was removed by centrifugation (2000 rpm for 10 min in a Beckman JA 4.2 rotor) and the radioactivity of a 400 μl aliquot of supernatant was quantified [48].

Measurement of k_{cat} for hydrolysis of GTP

$G_{i\alpha1}$ proteins (400 nM) were incubated at 30° C in 50 mM NaHEPES (pH 8.0), 5 mM EDTA, 3 mM DTT, 0.05 % Lubrol, and 1 μM [γ-^{32}P]GTP (7000 cpm pmole^{-1}) for 25 min. Reactions were then initiated by the addition of GTP and $MgSO_4$ to final concentrations of 100 μM and 10 mM, respectively. Aliquots were withdrawn at the indicated time intervals and counted as described for the steady-state GTPase assay [48]. Values of k_{cat} were calculated by a nonlinear least-squares fit to $B = B_{eq}(1–e^{–kt})$.

Measurement of Mg^{2+} affinity

$G_{i\alpha1}$ proteins (300 nM) were incubated at 30° C in 50 mM NaHEPES (pH 8.0), 5 mM EDTA, 5 mM DTT, 0.05 % Lubrol, and 10 μM GTPγS for 3 h. This mix was divided into 600 μl aliquots whereupon 6 μl of varying $MgSO_4$ solutions were added to generate aliquots with appropriate Mg^{2+} concentrations. Mg^{2+} binding was allowed to proceed for 15 min at room temperature. Measurements of the intrinsic tryptophan fluorescence were then recorded on a SPEX Fluorolog 211 spectrophotometer with excitation and emission wavelengths of 289 nm and 349 nm, respectively [30]. These data were fit into the equation: $F = ax/(d+x)$, where a is the maximum value F(x) and d is the dissociation constant.

Crystallization

GDP bound to G203AGia1 was replaced with GTPgS–Mg2+ by incubating the protein with 10 mM $MgSO_4$ and 1 mM GTPgS for 3 h at 30° C prior to crystallization. Crystals of G203AGia1 complexed with GDP–Pi were grown by the sitting drop method as described previously [28]. Briefly, sitting drops containing 10 μl G203AGia1 (10–20 mg ml^{-1}) activated with GTPgS–Mg^{2+}, 5 mM $MgSO_4$, 0.5 mM N-[2-hydroxethyl]-piperazine-N-[3-propanesulfonic acid] EDTA, 5 mM DTT, 5 mM GTPγS, 25 mM (NaEPPS) (pH 8.0) were mixed with 10 μl of a buffer containing ammonium phosphate (2.2–2.5 M, pH 5.5–5.8) and equilibrated against 1 ml of the same buffer. The sitting drops were incubated at 20° C. Crystals (space group P43212, a = b = 77.1 Å, c = 194.6 Å) of X-ray diffraction quality (0.3 mm × 0.3 mm × 1.0 mm) grew after 21–30 days. Crystals were mounted directly from the mother liquor just prior to data collection.

Data collection and processing

Data for the GDP complex of G203A$G_{i\alpha1}$ were measured and reduced as described [22]. Data for the GDP–Pi complex of G203A$G_{i\alpha1}$ were

Table 1

Data collection and refinement statistics.*

Parameter	GDP complex	GDP–Pi complex
Data collection		
Resolution range (Å)	40–2.6	40–2.6
Number of observations	58 681	28 864
Number of unique reflections	15 804	11 856
Completeness of data (%)		
All data	99.8	84.1
Highest shell (2.6–2.7 Å)	99.7	86.5
Observed reflections with $I/\sigma(I) > 2$ (%)		
All data	86.4	91.2
Highest shell	63.6	78.7
R_{merge} †		
All data	0.04	0.03
Highest shell	0.325	0.09
Final refinement parameters		
Resolution range (Å)	8.0–2.6	8.0–2.6
R factor (R_{free}) (%)		
All data	22.4 (28.9)	19.2 (28.3)
Highest shell	40.7 (47.3)	25.3 (35.0)
All data $I/\sigma(I) > 2$	21.7 (29.0)	18.2 (27.2)
Highest shell $I/\sigma(I) > 2$	36.1 (41.7)	22.0 (32.5)
Model parameters		
Number of protein atoms	3342	3138
Number of ligand atoms	45	45
Number of ordered waters	0	9
Rms deviations from ideal geometry		
Bond distances (Å)	0.013	0.011
Bond angles (°)	1.82	1.69
Improper torsions (°)	1.62	1.51
Ramachandran analysis‡		
Most favored (%)	92	89
Generous or disallowed (%)	0	0

*Statistics for G203A $G_{i\alpha1}$·GDP presented for completeness. The structure has been described elsewhere [22]. †$R_{merge} = \Sigma|I - <I>|/\Sigma <I>$. ‡Analysis using PROCHECK [54].

measured from a single crystal at room temperature on the F2 beamline at the Cornell High Energy Synchrotron Source (CHESS). The beamline was equipped with a Fuji imaging plate detector system. Detector images ($\Delta\phi = 1°$) were integrated with the program DENZO, and observations were merged and scaled with the SCALEPACK package [49]. Partial reflections were excluded in the data processing. Data collection statistics for both crystal forms are summarized in Table 1.

Molecular replacement and structure refinement

The determination and refinement of the $G203AG_{i\alpha1}$–GDP complex has been described [22]. Since that report, the model X-PLOR [50] sigmaA weighted $2F_o–F_c$ maps [51] were inspected, and polypeptide chain segments with poor electron density were deleted from the model. During the course of refinement most of the missing residues could be reintroduced into the model using the fitting program O [52]. The current model of the GDP bound form of $G203AG_{i\alpha1}$ contains 334 residues out of the 353 residues present in the protein (Met1 is cleaved). As in the wild type GDP–$G_{i\alpha1}$ structure, but unlike the wild type GTPγS–$G_{i\alpha1}$ structure, both the N and C-terminal domains are completely ordered except for residues 2–9. However, within the sequence two segments are disordered and have been modeled with zero occupancy (residues 236–239) or have been omitted from the model (residues 204–214). No electron density for these residues is observed in the final electron-density maps computed with refined phases and all data, including the low resolution shell. Quenching of tryptophan Trp211 fluorescence in the GDP-bound state suggests Switch II is solvent exposed and possibly disordered in solution (Fig. 1e). Furthermore, the side chains for 11 surface residues could not be unambiguously identified and their occupancy has been set to zero (residues 28, 90, 97, 102, 164, 216, 245, 256 312, 313 and 315). For two segments of polypeptide chain which flank a disordered region (residues 119–203 and residues 215–218), two conformations could be distinguished in electron-density maps, and have thus been modeled. Refinement statistics are summarized in Table 1.

The structure of the $203AG_{i\alpha1}$–GDP–Pi complex was determined by molecular replacement, again using coordinates for the $G_{i\alpha1}$–GTPγS–Mg^{2+} complex [18] as the search model. The correct orientation was obtained using the Patterson correlation refinement in X-PLOR [50] (the magnitude of the true solution was twice that of the first false peak). However, it was difficult to determine the exact position of the molecule in the asymmetric unit. Evaluation of the translation function in X-PLOR did not provide a satisfactory answer in either of the two enantiomorphic space groups $P4_12_12$ or $P4_32_12$. Therefore, a brute force approach was initiated using the program BRUTE

Figure 9

Simulated annealing omit map [50] of the active-site region surrounding GDP and Pi. Light blue colored contours correspond to F_o–F_c density in which the GDP, Pi and all protein residues and solvent molecules within 4.0 Å (residues 42, 43, 46, 178, 180, 181, 202, 203) were omitted from the phasing model. Dark blue contours represent density for the F_o–F_c omit map in which the Pi ion and residues 178–183, 200 and 202 were omitted from the model. Contours are shown for density at the 2 σ level.

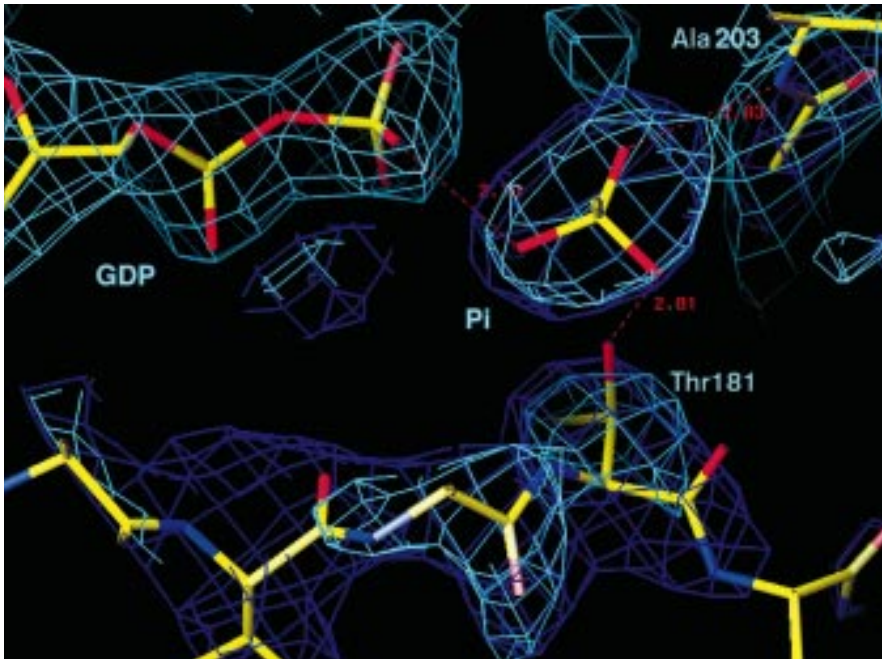

[53] which gave a clear solution in the space group $P4_32_12$. The strategy used for refinement was similar to that described for the G203AG$_{i\alpha1}$–GDP model [22]. During refinement, and prior to inclusion of the guanine nucleotide, density for a nucleotide could clearly be seen in electron-density maps, except for the γ-phosphate group. This indicated that the crystal structure contained bound GDP instead of GTPγS. In addition, 1.8 Å away from the expected site for a γ-phosphate, a strong peak of density was observed which was too large to be modeled as a water molecule. In the current model this density has been interpreted as a phosphate ion and has been refined as such. Figure 9 shows simulated annealing omit maps in which either Pi or GDP and Pi were removed from the final model. Pi appears as discrete density, sufficiently far from Thr181 to exclude autophosphorylation (which has never been observed in α subunits of heterotrimeric G proteins). Unlike the wild type G$_{i\alpha1}$–Mg^{2+}–GTPγS complex, no Mg^{2+} ion could be identified in the mutant structure. The final model contains the polypeptide chain from residues 32–348, the bound GDP nucleotide and one phosphate ion, as well as nine ordered water molecules. The N-terminal domain (residues 2–31) and the last six residues (residues 349–354) could not be observed in electron-density maps. The structure displays good stereochemistry with 89% of the residues in the most favored regions of the Ramachandran distribution, 11% in additional allowed regions and none in generous or disallowed regions, as defined in PROCHECK [54]. Refinement statistics are given in Table 1.

Accession numbers

Coordinates and structure factors for the G203G$_{i\alpha1}$–GDP–Pi complex are available from the Protein Databank with accession code 1GIT.

Acknowledgements

We are grateful to David Coleman, Mark Mixon, Bryan Sutton, Jim Naismith, and the staff at the Cornell High Energy Synchrotron Source (CHESS) for assistance with data collection. This work was supported by National Institutes of Health (NIH) grant DK46371 and Welch Foundation grant I-1229 (to SRS) and NIH grant GM34497, American Cancer Society grant BE30-O, Welch Foundation grant I-1271, and the Raymond and Ellen Willie Chair of Molecular Neuropharmacology (to AAG).

References

1. Gilman, A.G. (1987). G proteins: transducers of receptor-generated signals. *Annu. Rev. Biochem.* **56**, 615–649.
2. Hepler, J.R. & Gilman, A.G. (1992). G proteins. *Trends Biochem. Sci.* **17**, 383–387.
3. Bourne, H.R., Sanders, D.A. & McCormick, F. (1991). The GTPase superfamily: conserved structure and molecular mechanism. *Nature* **349**, 117–127.
4. Bourne, H.R., Sanders, D.A. & McCormick, F. (1990). The GTPase superfamily: a conserved switch for diverse cell functions. *Nature* **348**, 125–132.
5. Kaziro, Y., Itoh, H., Kozasa, T., Nakafuku, M. & Satoh, T. (1991). Structure and function of signal-transducing GTP-binding proteins. *Annu. Rev. Biochem.* **60**, 349–400.
6. Barbacid, M. (1987). *ras* Genes. *Annu. Rev. Biochem.* **56**, 779–827.
7. Kjeldgaard, M. & Nyborg, J. (1992). Refined structure of elongation factor EF-Tu from *Escherichia coli*. *J. Mol. Biol.* **223**, 721–742.
8. Berchtold, H., Reshetnikova, L., Reiser, C.O.A., Schirmer, N.K., Sprinzl, M. & Hilgenfeld, R. (1993). Crystal structure of active elongation factor Tu reveals major domain rearrangements. *Nature* **365**, 126–132.
9. Czworkowski, J., Wang, J., Steitz, T.A. & Moore, P.B. (1994). The crystal structure of elongation factor G complexed with GDP, at 2.7 Å resolution. *EMBO J.* **13**, 3661–3668.
10. AEvarsson, A., *et al.*, & Liljas, A. (1994). Three-dimensional structure of the ribosomal translocase: elongation factor G from *Thermus thermophilus*. *EMBO J.* **13**, 3669–3677.
11. De Vos, A.M., *et al.*, & Kim, S.-H. (1988). Three-dimensional structure of an oncogene protein: catalytic domain of human c-H-*ras* p21. *Science* **239**, 888–893.
12. Pai, E.F., Kabsch, W., Krengel, U., Holmes, K.C., John, J. & Wittinghofer, A. (1989). Structure of the guanine-nucleotide-binding domain of the Ha-*ras* oncogene product p21 in the triphosphate conformation. *Nature* **341**, 209–214.
13. Milburn, M.V., *et al.*, & Kim, S.-H. (1990). Molecular switch for signal transduction: structural differences between active and inactive forms of protooncogenic Ras proteins. *Science* **247**, 939–945.
14. Scheffzek, K., Klebe, C., Fritz-Wolf, K., Kabsch, W. & Wittinghofer, A. (1995). Crystal structure of the nuclear Ras-related protein Ran in its GDP-bound form. *Nature* **374**, 378–381.
15. Amor, J.C., Harrison, D.H., Kahn, D.H. & Ringe, D. (1994). Structure of the human ADP-ribosylation factor 1 complexed with GDP. *Nature* **372**, 704–708.

16. Noel, J.P., Hamm, H.E. & Sigler, P.B. (1993). The 2.2 Å crystal structure of transducin-α complexed with GTPγS. *Nature* **366**, 654–663.
17. Lambright, D.G., Noel, J.P., Hamm, H.E. & Sigler, P.B. (1994). Structural determinants for activation of the α subunit of a heterotrimeric G protein. *Nature* **369**, 621–628.
18. Coleman, D.E., Berghuis, A.M., Lee, E., Linder, M.E., Gilman, A.G. & Sprang, S.R. (1994). Structures of active conformations of $G_{i\alpha1}$ and the mechanism of GTP hydrolysis. *Science* **265**, 1405–1412.
19. Eccleston, J.F. & Webb, M.R. (1982). Characterization of the GTPase reaction of elongation factor Tu. *J. Biol. Chem.* **257**, 5046–5049.
20. Feuerstein, J., Goody, R.S. & Webb, M.R. (1989). The mechanism of guanosine nucleotide hydrolysis by p21 c-Ha-*ras*. *J. Biol. Chem.* **264**, 6188–6190.
21. Sondek, J., Lambright, D.G., Noel, J.P., Hamm, H.E. & Sigler, P.B. (1994). GTPase mechanism of G proteins from the 1.7 Å crystal structure of transducin α GDPAlF_4. *Nature* **372**, 276–279.
22. Mixon, M.B., Lee, E., Coleman, D.E., Berghuis, A.M., Gilman, A.G. & Sprang, S.R. (1995). Tertiary and quaternary structural changes in $G_{i\alpha1}$ induced by GTP hydrolysis. *Science* **270**, 954–960.
23. Northup, J.K., Smigel, M.D., Sternweis, P.C. & Gilman, A.G. (1983). The subunits of the stimulatory regulatory component of adenylate cyclase. Resolution of the activated 45,000-dalton α subunit. *J. Biol. Chem.* **258**, 11369–11376.
24. Salomon, M.R. & Bourne, H.R. (1981). Novel S49 lymphoma variants with aberrant cyclic AMP metabolism. *Mol. Pharmacol.* **19**, 109–116.
25. Bourne, H.R., Kaslow, D., Kaslow, H.R., Salomon, M.R. & Licko, V. (1981). Hormone-sensitive adenylate cyclase. Mutant phenotype with normally regulated beta-adrenergic receptors uncoupled with catalytic adenylate cyclase. *Mol. Pharmacol.* **20**, 435–441.
26. Miller, R.T., Masters, S.B., Sullivan, K.A., Beiderman, B. & Bourne, H.R. (1988). A mutation that prevents GTP-dependent activation of the α chain of G_s. *Nature* **334**, 712–715.
27. Lee, E., Taussig, R. & Gilman, A.G. (1992). The G226A mutant of $G_{s\alpha}$ highlights the requirement for dissociation of G protein subunits. *J. Biol. Chem.* **267**, 1212–1218.
28. Coleman, D.E., *et al.*, & Sprang, S.R. (1994). Crystallization and preliminary crystallographic studies of $G_{i\alpha1}$ and mutants of $G_{i\alpha1}$ in the GTP and GDP-bound states. *J. Mol. Biol.* **238**, 630–634.
29. Lee, E. (1994). The structural basis of G protein activation. PhD Dissertation. The University of Texas Southwestern Medical Center, Dallas, USA.
30. Higashijima, T., Ferguson, K.M., Sternweis, P.C., Ross, E.M., Smigel, M.D. & Gilman, A.G. (1987). The effect of activating ligands on the intrinsic fluorescence of guanine nucleotide-binding regulatory proteins. *J. Biol. Chem.* **262**, 752–756.
31. Fung, B.K.-K. & Nash, C.R. (1983). Characterization of transducin from bovine retinal rod outer segments. II. Evidence for distinct binding sites and conformational changes revealed by limited proteolysis with trypsin. *J. Biol. Chem.* **258**, 10503–10510.
32. Ueda, N., Iñiguez-Lluhi, J.A., Lee, E., Smrcka, A.V., Robishaw, J.D. & Gilman, A.G. (1994). G protein βγ subunits: simplified purification and properties of novel isoforms. *J. Biol. Chem.* **269**, 4388–4395.
33. Wall, M.A., *et al.*, & Sprang, S.R. (1995). The structure of the protein heterotrimer $G_{i\alpha1}\beta\gamma$. *Cell* **80**, 1047–1058.
34 Wilmot, C.M. & Thornton, J.M. (1990). β-Turns and their distortions: a proposed new nomenclature. *Protein Eng.* **3**, 479–493.
35. Lambright, D.G., Sondek, J., Bohm, A., Skiba, N.P., Hamm, H. & Sigler, P.B. (1996). The 2.0 Å crystal structure of a heterotrimeric G protein. *Nature* **379**, 311–319.
36. Brandt, D.R. & Ross, E.M. (1986). Catecholamine-stimulated GTPase cycle. *J. Biol. Chem.* **261**, 1656–1664.
37. Maegley, K. A., Admiraal, S.J. & Herschlag, D. (1996). Ras-catalyzed hydrolysis of GTP: a new perspective from model studies. *Proc. Natl. Acad. Sci. USA.* **93**, 8160–8166.
38. Privé, G.G., *et al.*, & Kim, S.-H. (1992). X-ray crystal structures of transforming p21 *ras* mutants suggest a transition-state stabilization mechanism for GTP hydrolysis. *Proc. Natl. Acad. Sci. USA* **89**, 3649–3653.
39. Schweins, T., Langen, R. & Warshel, A. (1994). Why have mutagenesis studies not located the general base in *ras* p21. *Nat. Struct. Biol.* **1**, 476–484.
40. Schweins, T., Geyer, M., Scheffzek, K., Warshel, A., Kalbitzer, H.R. & Wittinghofer, A. (1995). Substrate-assisted catalysis as a mechanism for GTP hydrolysis of $p21^{ras}$ and other GTP-binding proteins. *Nat. Struct. Biol.* **2**, 36–44.
41. Mittal, R., Ahmadian, M.H., Goody, R.S. & Wittinghofer, A. (1996). Formation of a transition-state analog of the *ras* GTPase reaction by Ras·GTP, tetrafluoroaluminate, and GTPase-activating proteins. *Science* **273**, 115–117.
42. Brownbridge, G.G., Lowe, P.N., Moore, K.J., Skinner, R.H. & Webb, M.R. (1993). Interaction of GTPase activating proteins (GAPs) with p21*ras* measured by a novel fluorescence anisotropy method. Essential role of ARG-903 of GAP in activation of GTP hydrolysis on p21ras. *J. Biol. Chem.* **268**, 10914–10919.
43. Markby, D.W., Onrust, R. & Bourne, H.R. (1993). Separate GTP binding and GTPase activating domains of a Gα subunit. *Science* **262**, 1895–1901.
44. Berman, D.M., Wilke, T.M. & Gilman, A.G. (1996). GAIP and RGS4 are GTPase-activating proteins (GAPs) for the G_i subfamily of G protein α subunits. *Cell* **86**, 1–20.
45. Berman, D.M., Kozasa, T. & Gilman, A.G. (1996). The GTPase-activating protein RGS4 stabilizes the transition state for nucleotide hydrolysis. *J. Biol. Chem.* in press.
46. Lee, E., Linder, M.E. & Gilman, A.G. (1994). Expression of G protein α subunits in *Escherichia coli*. *Methods Enzymol.* **237**, 146–164.
47. Northup, J.K., Smigel, M.D. & Gilman, A.G. (1982). The guanine nucleotide activating site of the regulatory component of adenylate cyclase. Identification by ligand binding. *J. Biol. Chem.* **257**, 11416–11423.
48. Higashijima, T., Ferguson, K.M., Smigel, M.D. & Gilman, A.G. (1987). The effect of GTP and Mg^{2+} on the GTPase activity and the fluorescent properties of Go. *J. Biol. Chem.* **262**, 757–761.
49. Otwinowski, Z. (1993). Oscillation Data Reduction Program. In *Proceedings of the CCP4 Study Weekend: Data collection and Processing*. (Sawyer, L., Isaacs, N. & Bailey, S., eds), pp.56–62, Daresbury Laboratory, Warrington, UK.
50. Brünger, A.T. (1992). *X-PLOR, Version 3.1: a system for X-ray crystallography and NMR*. Yale University Press, New Haven, CT, USA.
51. Read, R.J. (1986). Improved Fourier coefficients for maps using phases from partial structures with errors. *Acta Cryst. A* **42**, 140–149.
52. Jones, T.A. & Kjeldgaard, M.O. (1993). *O Version 5.9*. Department of Molecular Biology, Uppsala University, Uppsala, Sweden.
53. Fujinaga, M. & Read, R.J. (1987). Experiences with a new translation-function program. *J. Appl. Cryst.* **20**, 517–521.
54. Laskowski, R.A., MacArthur, M.W., Moss, D.S. & Thornton, J.M. (1993). PROCHECK: a program to check the stereochemical quality of protein structures. *J. Appl. Cryst.* **26**, 283–291.
55. Evans, S.V. (1993). SETOR: hardware lighted three-dimensional solid model representations of macromolecules. *J. Mol. Graph.* **11**, 134–138.
56. Bernstein, F.C., *et al.*, & Tasumi, M. (1977). The protein databank: a computer-based archival file for macromolecular structure. *J. Mol. Biol.* **112**, 535–542.